water

MDPI

Article

Environmental Assessment Impact of Acid Mine Drainage from Kizel Coal Basin on the Kosva Bay of the Kama Reservoir (Perm Krai, Russia)

Evgeniya Ushakova *, Elena Menshikova, Sergey Blinov, Boris Osovetsky and Pavel Belkin

Department of Geology, Perm State University, Bukireva St. 15, 614990 Perm, Russia; menshikova_e@list.ru (E.M.); blinov_s@mail.ru (S.B.); opal@psu.ru (B.O.); pashabelkin@mail.ru (P.B.)
* Correspondence: ushakova.evgeniya@gmail.com; Tel.: +7-919-704-7507

Abstract: The Kosva Bay is permanently affected by acid mine drainage (AMD) from Kizel Coal Basin in the Perm Krai of Russia. This discharge is released in the middle part of the Kosva River from the abandoned mines. This study investigates the current trace element (TE) concentrations for Zn, Cu, Pb, Ni, Cr, Cd, As, and Hg and the mineral composition, major oxides, grain size of sediments, and acute toxicity using two test organisms within the site of AMD downstream from the Kosva River and up to the Kosva Bay of Kama Reservoir. The objectives of this study were to analyze the quality of sediment and level pollution of Kosva Bay using pollution and ecotoxicological indices. The environmental indices, namely the contamination factor (*CF*), the geoaccumulation index (I_{geo}), and the potential ecological risk factor (E_r^i), indicate contamination by Cr and Pb in sediments at the site of AMD, with the highest values for Cr, Cu, and As in the Kosva Bay sediments downstream of abandoned coal mines. The results of I_{geo} and *CF* average values in bay of sediments showed different degrees of contamination, from moderate contamination to considerable contamination, respectively. According to the potential ecological risk index (RI) values, the Kosva Bay sediments exhibited low to moderate risk, and As and Cd have the highest contribution rate. According to LAWA and the Polish geochemical classification of sediments, sediments of the bay correspond to the highest levels (IV–III classes) for Cr, Ni, and Hg. Based on the SQG_C, Hg, Cd, Cr, and Ni are the most probable for resulting in adverse effects on aquatic organisms in this study. The results of this study indicate that complex pollution and ecotoxicological indices must be supported by ecotoxicologal tests. High precipitation totals, low evaporation rates, and flow regulation stream by the Shirokovsky Reservoir located upstream from abandoned coal mines provide significant fluctuations in streamflow, which is probably the most important factor controlling the distribution and mobility of TE in the studied sediments.

Keywords: trace elements; acid mine drainage; Kizel Coal Basin; sediments; pollution; ecotoxicity

Citation: Ushakova, E.; Menshikova, E.; Blinov, S.; Osovetsky, B.; Belkin, P. Environmental Assessment Impact of Acid Mine Drainage from Kizel Coal Basin on the Kosva Bay of the Kama Reservoir (Perm Krai, Russia). *Water* **2022**, *14*, 727. https://doi.org/10.3390/w14050727

Academic Editor: Domenico Cicchella

Received: 21 January 2022
Accepted: 19 February 2022
Published: 24 February 2022

1. Introduction

Acid mine drainage (AMD) has become a serious, worldwide environmental problem for river ecosystems caused by mining operations and abandoned coal mines [1,2]. Adverse effects on the abiotic and biotic components of rivers, including the destruction of aquatic life, bioaccumulation of toxic elements by organisms and plants, biodiversity loss, and the health of local residents, are observed for these areas [3–6]. AMD of abandoned coal mines is the source of river water pollution in the area of Moscow Brown Coal Basin and Kizel Coal Basin of Russia [7–9]; Tinto and Odiel Rivers in Spain [10]; Leonor and Pedras streams in a coal mining area (southern Brazil) [11]; rivers of Central Appalachian, Eastern State, and the Great Plains regions of the United States [12]; and many rivers in other regions [13–15]. Surface water pollution with AMD associated with coal mining areas are caused by oxidative processes of mine waters due to oxidation of sulfide group minerals,

resulting in the release of large amounts of sulfates, iron, and trace elements (TE) (e.g., As, Cd, Co, Cu, Pb, Zn, Al, Mn, Be) [16–18].

In order to understand the potential environmental hazards of pollutants in river basins, sediments must be evaluated. It has been established that approximately 99% of TE in aquatic systems eventually settles in sediments, forming concentrations that are four to five times higher than those in the overlying water [19].

Abandoned mines in the Kizel Coal Basin, located in the eastern Perm Krai (Russia), have been responsible for seriously affects on watersheds of the Yaiva, Kosva, Us'va, and Vilva rivers and their tributaries due to AMD and runoff from the tailing deposits. The outflow of AMD from the mines of Kizel Coal Basin occurs in 19 sources, with an average discharge during the period 2007–2013 of about 25,000 m^3/h. The AMD is characterized by pH 2–3, high salinity (up to 35 g/L), and large amounts of sulfate (up to 15,681 mg/L), Fe (up to 3500 mg/L), Al (up to 225 mg/L), Mn (up to 215 mg/L), and some TE (Be, Co, Ni, Li, Pb, Zn) [18,20]. It is formed as a result of interaction of groundwater of flooded mines of the basin with the rocks of the coal layers, which contain high concentrations of sulfur up to 12–15% [21]. Many elements are found in higher concentrations in sediments within AMD areas. For example, in the sediments of the Kosva River the Fe content reaches Fe—197,991 mg/kg, Al—12,100 mg/kg, Mn—156.4 mg/kg, Zn—49.99 mg/kg, Li—24.78 mg/kg, Ni—25.36 mg/kg, Pb—14.57 mg/kg, Co—6.09 mg/kg, and Cd—0.162 mg/kg [20]. Nieto et al. [22] and Adamovic et.al. [23] noted pollutant transport over significant distances from AMD [22,23]. The total amount of pollutants from mine outflow from the Kizel Coal Basin (for the catchment areas of the Yaiva, Kosva, and Chusovaya Rivers) is 21,455 tons per year of iron, 1128 tons per year of aluminum, and 217 tons per year of manganese [24]. The Kosva River basin, including Kosva Bay of Kama Reservoir, is an attractive site in the Ural foothills that is used for recreation (such as rafting, fishing) by the local population. In this regard, a complex assessment of the contamination level of river sediments with toxic elements and compounds has an important scientific and practical value, as it provides useful information for a comparative assessment of this territory and other areas that are adversely impacted by AMD.

The key to the effective assessment of sediment contamination with TE lies in the use of different pollution and ecotoxicological indices [25–27]. The pollution indices can be divided into three groups: individual and complex indices as well as quality guidelines or geochemical classifications. The content of each individual TE in sediments is calculated using the individual and ecotoxicological indices. The values of geoaccumulation index (I_{geo}), enrichment factor (EF), single-pollution index (PI), contamination factor (*CF*), and potential ecological risk factor (E_r^i) can be used to classify sediments into several classes based on pollution level [28–34]. Complex pollution and ecotoxicological indices (sum of contamination (PI_{sum}), Nemerow pollution index ($PI_{Nemerow}$), pollution load index (*PLI*), average single-pollution index (PI_{avg}), background enrichment factor (PIN), multi-element contamination (MEC), contamination security index (CSI), degree of contamination (Cdeg), and potential ecological risk (RI)) are used to determine sediment contamination based on the content of more than one TE or a sum of individual indices [34–39]. To assess the level of contamination to predict adverse ecological effect living organisms, it is common to apply ecotoxicological criteria or use indicators (sediment quality guidelines (SQGs), LAWA classifications, and geochemical classification of aquatic sediments by Bojakowska) that take into account the level of metal toxicity [40–43]. The SQGs, LAWA, and geochemical classification quotients are widely used by researchers and environmental managers to determine the indicative toxicity sediments as a simple and easily understandable numerical index based on ecotoxicological effect on benthic organisms in freshwater ecosystems [44,45]. As different techniques are used in the calculation of pollution and ecotoxicological indices, a complex approach is recommended to avoid confusion and uncertainty during the sediment quality assessment [46,47].

Bioassays are a useful tool for ecological risk assessment of the level of sediment contamination [48–51]. They are a good addition to chemical analysis, as they thoroughly

describe the accumulation of toxic elements in sediments as well as their bioavailability and interaction [52–54]. This testing is widely used in the environmental assessment of sediments affected by AMD with low pH values, high sulfate, and TE concentrations [55–57]. Studies in South Korea using *Daphnia magna* to assess the adverse effects of AMD show that acidic pH directly affects the growth of *Daphnia magna* and can also dramatically increase their mortality at pH < 3.7 [58]. In this study, it was found that the toxicity depended on the concentration of certain elements, such as Cd, Cu, Mn, and Zn. However, the actual toxicity of AMD depends on the processes of sedimentation of large amounts of iron by formation of amorphous iron sediment and the process of sorption of metals on it.

The purpose of this study is to assess the current condition of the Kosva Bay sediments affected by AMD and runoff from mine waste rock dumps of the Kizel Coal Basin. The Kosva River and the Kosva Bay have been assessed at their confluence with the Kama Reservoir.

The present study has the following aims:

- To determine mineral and granulometric composition of sediments;
- To identify the basic distribution of the major and TE of sediments;
- To assess the potential ecological risk of TE in sediments using SQGs, LAWA, *CF*, *PLI*, I_{geo}, RI, and PECQ;
- To assess sediment toxicity at the most representative sites using bioassays (with *Daphnia magna* and *Scenedesmus quadricauda* Breb.) and to also evaluate calculated pollution indices.

2. Site Description

2.1. Hydrology and Climatology

The Kosva Bay is located in Perm Krai, Russia, between 58°52′ and 58°56′ north latitude and 56°19′ and 56°40′ east longitude. The Kosva River originates on the western slope of the Middle Urals and then enters the Pre-Urals plain. The watercourse length is 310 km, and the drainage basin is 7485 km^2. The Kosva River watershed has an average elevation of 351 m, with the highest elevations over 1569 m above Baltic Sea level in the western, mountainous part of the Middle Urals. Approximately 60% of the watershed has elevation between 250 and 700 m and less than 1% more than 700 m. The level regime of the Kosva River in its middle course is influenced by the operation of Shirokovskaya HES, while the estuarial part of the river is in backwater of the Kama Reservoir. There are several residential areas along the Kosva River, the largest of which is Gubakha, with a population of 19,000 people.

The amount of rainfall in the Kosva watershed from May 2020 to April 2021 was 772.5 mm (Figure 1). The average temperature for the observation period is 0.8 °C, with minimum and maximum values of −19.0 °C and 19.5 °C, respectively. Multi-year data from Perm Centre of Hydrometeorology and Monitoring of Environment of air average annual temperature in the area under study comprise 0.5 °C with variation from −52 °C to +34 °C [59]. The mean streamflow of the Kosva River at Peremskoe for the observation period is 92.0 m^3/s, which corresponded to the multi-year values: maximal expenditure—122 m^3/s; minimal expenditure—53.1 m^3/s [60].

2.2. Geology

The geological structure of the Kosva River basin is described using the general chronostratigraphic scale as of 2019, in accordance with the Stratigraphic Code of Russia 2019 and the adopted MSC Resolutions . . . 2012, 2013, 2016. The West Ural folding zone, within which the Kizel Coal Basin is located, is in the eastern part of the study area and has the fold-uplift-thrust structure (Figure 2). The Kizel Coal Basin includes Paleozoic sedimentary rocks from the Lower Devonian to the Artinskian stage (Lower Permian), with a total thickness of 3000–4000 m [61]. The area in the eastern part of the Shirokovsky Reservoir within the Middle Urals is composed of Upper Vendian rocks [62]. The place of the Vendian in the International Chronostratigraphic Scale corresponds to the upper series of the Ediacaran System [63,64]. The lower part of the watershed drains rocks of the Kungurian

and Ufimian stages (Lower Permian) with overlying Quaternary sediments of the east of the East European Plain. There is currently a problem with the stratigraphic location and self-sufficiency of the Ufimian stage (and its subdivisions—the Solikamsk and Sheshma horizons) [65–67]. Some researchers include the Sheshma horizon within the Kazanian Stage (corresponding to the Rodian Stage). At the same time, the Solikamsk Horizon is included in the Kungurian Stage (Leonardian Stage) [68,69]. According to Plyusnin et al. [67], the Ufimian Stage should be classified as the middle of the Permian system.

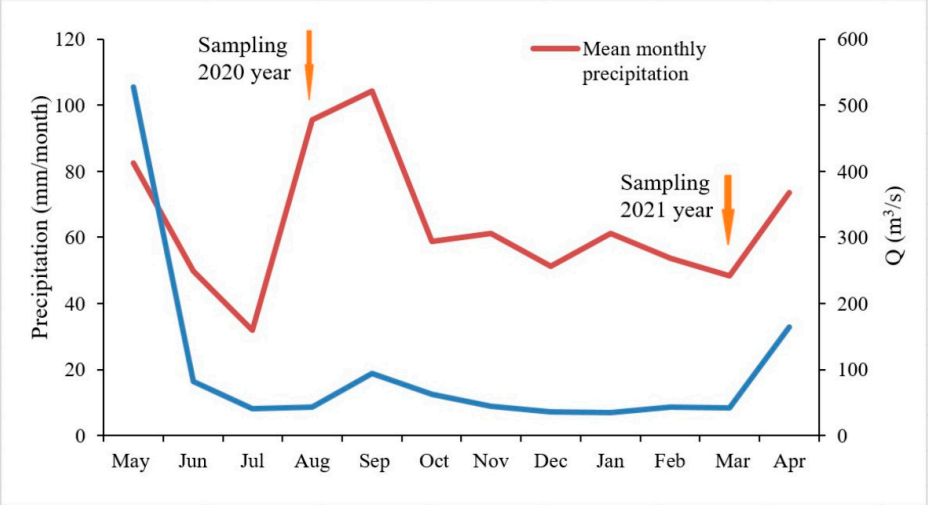

Figure 1. Mean monthly precipitation at Gubakha weather station and mean monthly streamflow at hydrological station Peremskoe (data period May 2020–April 2021).

The coal-bearing strata (Viseian stage of the Lower Carboniferous) of the Kizel Coal Basin is formed by sandstones, siltstones, mudstones, and clay shales with interlayers of limestones. The rocks of the coal-bearing strata include finely dispersed pyrite and organic sulfur. The content of sulfide and organic sulfur reaches 12–15%. Sulphur is one of the main active elements of the coal-bearing strata, determining the acid-alkaline and redox conditions of sediment accumulation, the concentration of TE on the hydrogen sulfide geochemical barrier, and their leaching in the oxidation zone with the formation of products that affect the environmental condition of the area [21].

The Kosva River flows throughout a region with well-developed karst processes (28–29% of the river basin territory). Surface discharge is either partially or completely captured by karst funnels, resulting in the formation of dry lands across a vast portion of the valley. Following the karst cavities, the waters are discharged as springs in the river valley [60].

2.3. Hydrogeology

Hydrogeologically, the eastern part of Perm Krai is related to the Bolsheuralsky complex formation water basin. The aquifers in Kizel Coal Basin can be divided into two aquifer systems: Quaternary aquifer and Lower Carboniferous–Lower Permian limestone karst fissure aquifer [60]. Quaternary aquifer is associated with river alluvium and alluvial–diluvial sandy clay and loams. Due to the insignificant area of distribution and low thickness, groundwater of quaternary deposits is not used for water supply. Lower Carboniferous–Lower Permian karst fissure aquifer is within the Kizel Coal Basin area, which includes two aquifers: the Carboniferous Moskovian Formation–Permian Artinskian Formation and the Carboniferous Vizean Formation–Bashkirian Formation. Flooding of abandoned mine fields resulted in the formation of technogenic aquifer of mine waters within coal-bearing strata. The groundwater aquifer related to the Carboniferous Vizean Formation–Bashkirian Formation is involved in the watering of most mines within the Kizel Coal Basin. In addition, it is a major source of AMD in the Kosva River basin [61].

Due to the drainage influence of underground mining works on the hydrodynamic regime of the Carboniferous Vizean Formation–Bashkirian Formation aquifer, the groundwater movement of this aquifer is oriented not in the direction of natural areas of discharge but in the direction of mine workings. The Carboniferous Vizean Formation–Bashkirian Formation aquifer is supplied mainly by absorption of rainwater and meltwater by numerous karst sinkholes in the development area of the aquifer. A large amount of rainfall, twice as much as evaporation, and widespread distribution of Carboniferous Vizean Formation–Bashkirian Formation contribute to the formation of significant natural resources of the aquifer [70].

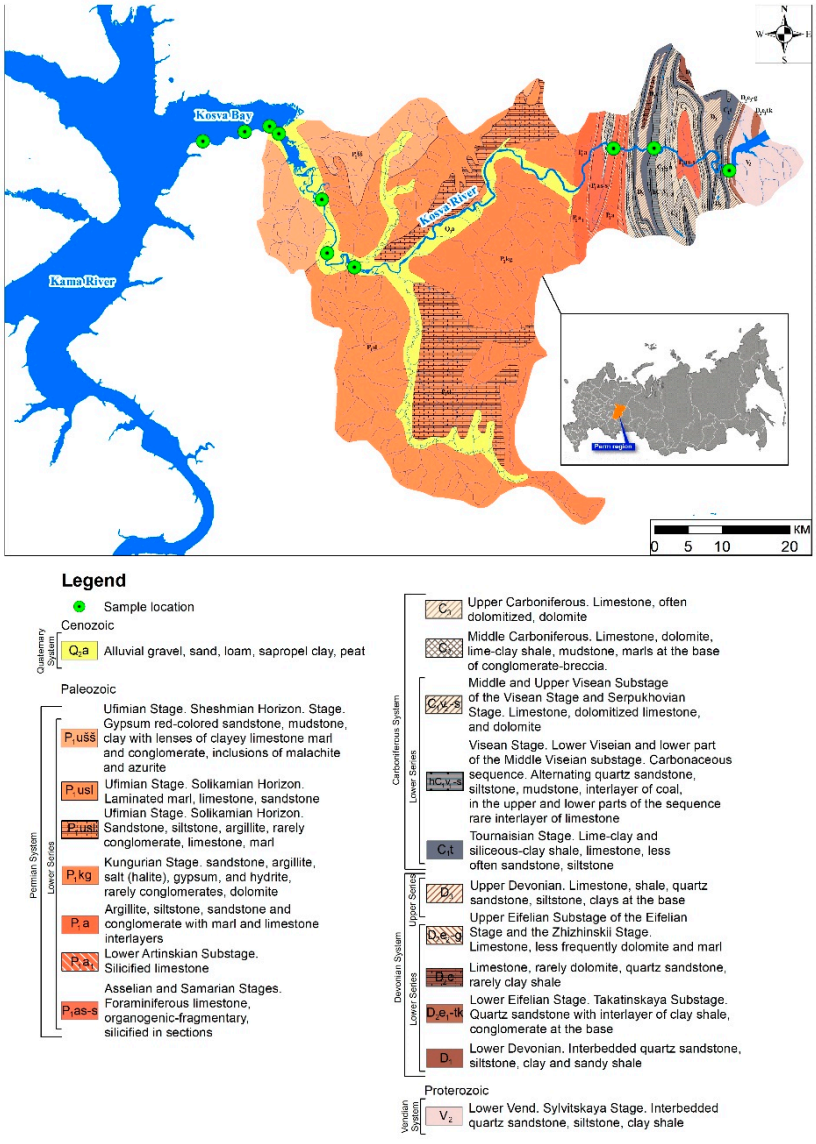

Figure 2. Geological map of the study area with the location of the sampling points.

2.4. AMD Characteristics

Kosva River flows through the territory of Kizel Coal Basin for 20 km in the middle part of the watershed. AMD outflow from coal mines, which were closed in the early 2000s, occurs within the basin of this river both into its small tributaries—Shumikha, Gubashka, Ladeiny Log, Berestyanka, and Kamenka—and into the Kosva River (Figure 3). Uncontrolled inflow of mine waters in the Kosva River basin from five terminated mines comprises nearly 9.8 million m^3/y. It results in the formation of significant amount of precipitates of ferrum and aluminum hydroxides. These sediments actively interact with

river water, contaminating rivers for many kilometers downstream, and enter the Kama Reservoir [60].

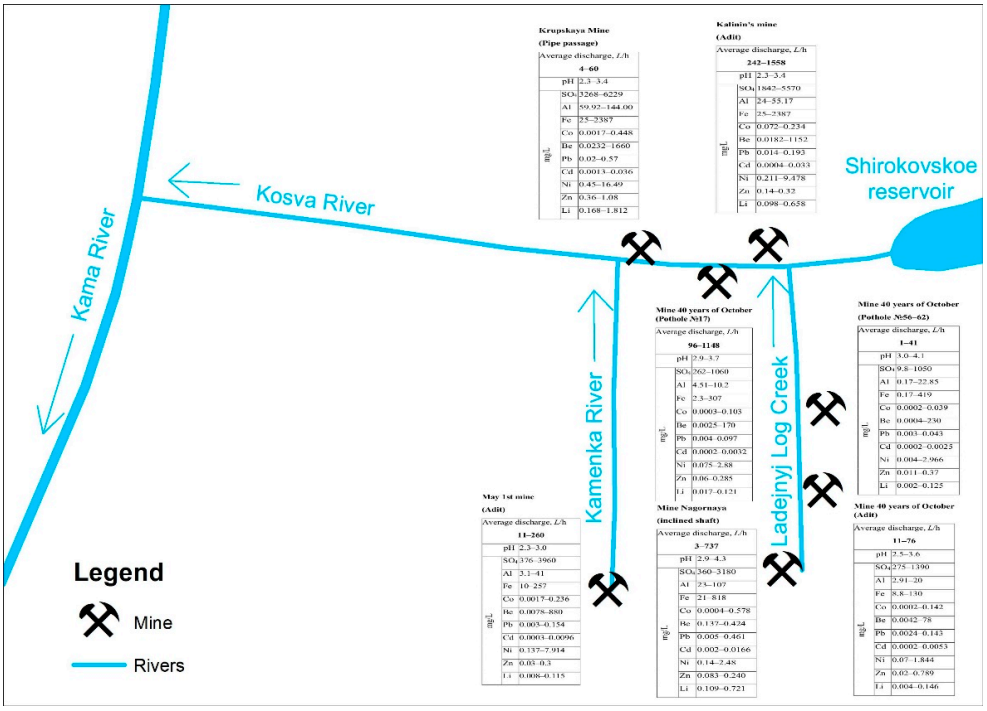

Figure 3. Location scheme and characteristics of AMD discharge in the Kosva River basin for the period from 2013 to 2019 [20].

Mine waters discharged in the Kosva River basin are characterized by acidic reaction (pH 2.3–4.3), high mineralization (up to 13 g/L), and significant contents of sulfates (up to 6229 mg/L), iron (up to 2387 mg/L), aluminum (up to 144 mg/L), and a number of TE (Be, Co, Ni, Li, Pb, and Zn) (Figure 3).

During the observation period from 2013 to 2019, the greatest AMD was noted from the Kalinin mine adit and pit No. 17 of the mine named "40 let Oktyabrya" ("40 years of October"); the discharge rates were 242–1558 L/s and 96–1148 L/s, respectively. AMD from the Krupskaya Mine and Kalinin Mine had the highest level of pollution, with iron concentrations reaching 2387 mg/L during the abovementioned observation period [20].

3. Materials and Methods

3.1. Field and Laboratory Analysis

Sediment samples were collected from six sampling points from upstream (R1) to downstream (R6) of the Kosva River and four samples in Kosva Bay (B1–B4) (Figure 4). Sampling point R1 was considered as a control for the Kosva River because it is located upstream of the AMD. Using a patented core sampler (RU 2762631C1, registration date 21 December 2021), sediments from the Kosva River were sampled in August 2020 and in the Kosva Bay during the winter low-water period of 2021 from the ice. Samples collected with the core sampler were analyzed to a depth of 0.20 m and were the most interesting in terms of potential effects on water quality. Table 1 shows the location of the sampling points.

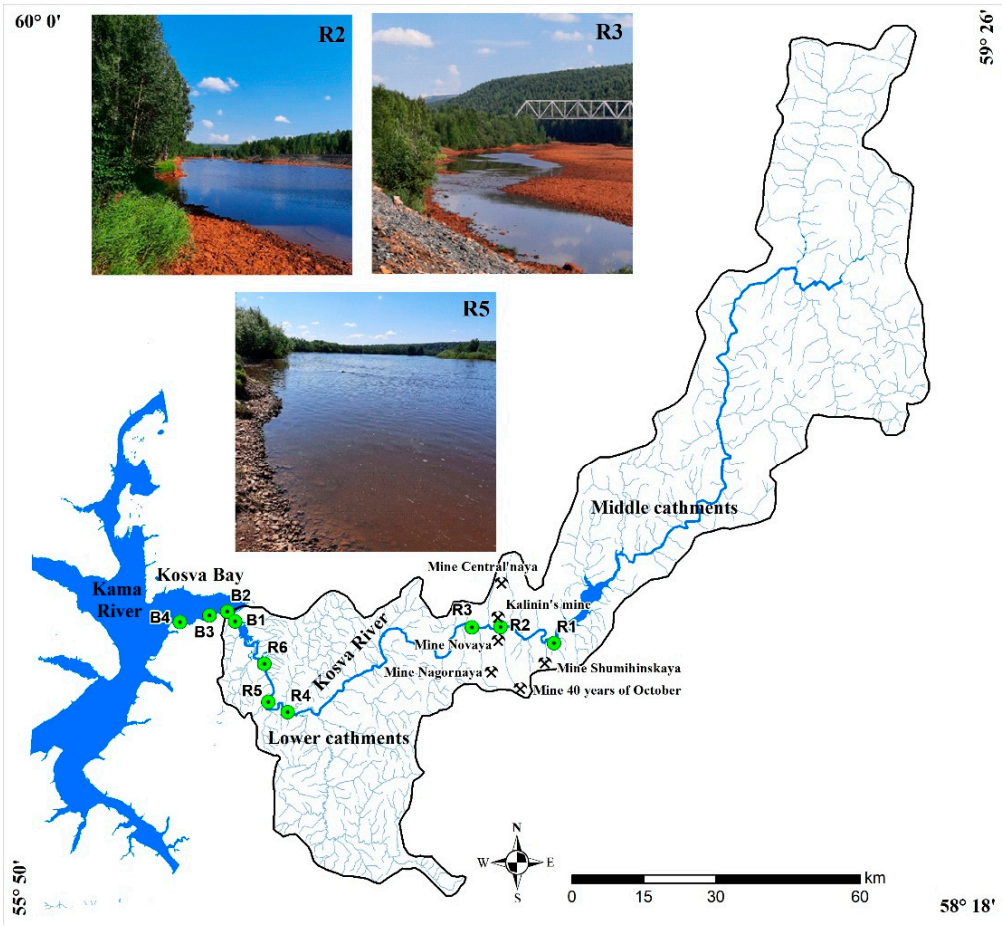

Figure 4. Kosva River drainage basin with sampling points.

Table 1. Location of sampling points.

Sampling Point	Latitude (N)	Longitude (E)	Height (m B.H.S.)	Distance from AMD (km)
R1	58°50′5.44″	57°47′9.51″	172	−16.8
R2	58°51′56.77″	57°35′39.31″	158	0.1
R3	58°51′56.50″	57°29′25.27″	148	2.3
R4	58°42′30.73″	56°49′38.38″	115	58.5
R5	58°47′53.87″	56°44′36.51″	110	73.9
R6	58°43′38.82″	56°45′28.11″	112	65.1
B1	58°52′38.00″	56°38′14.59″	108	78.3
B2	58°53′43.22″	56°36′30.86″	108	81.3
B3	58°53′16.98″	56°32′43.08″	108	85.1
B4	58°52′30.48″	56°26′17.07″	108	91.4

The concentration of Zn, Cu, Pb, Ni, Cr, Cd, As, and Hg were measured using the Aurora M90 ICP-MS spectrometer (Bruker, Fremont, CA USA). Sample preparation before ICP-MS measurements was brought into a solution by autoclave digestion. To obtain an efficient digestion, sediment was used with various acids or mixtures, such as concentrated HNO_3 or other acids (such as HCl, $HClO_4$, and H_2SO_4) or H_3BO_3 solution diluted with deionized water. For the analysis, we used 0.1-g sample weights. Together with the analyzed samples, control samples (blank samples) and one standard sample were decomposed. Standard samples from the Institute of Geochemistry, Siberian Branch of the Russian Academy of Sciences (Irkutsk, Russia) were used to ensure the accuracy of the

sample analysis. Validity of the analytical methods was confirmed by the analysis of the standard reference material Gabbro Essexit STD-2A (GSO 8670-2005).

Mineral analysis of major oxides (SiO_2, Al_2O_3, Fe_2O_3, CaO, MgO, TiO_2, Na_2O, K_2O, TiO_2, MnO, P_2O_5, and SO_3) was determined using X-ray diffraction (XRD) analysis Bruker D2 diffractometer. Loss on ignition (LOI) was determined by the weight loss upon heating a 1 g split sample at 950 °C for 90 min. The samples were pre-dried at room temperature, and then, approximately 2 g of sediment was pulverized with pestle and mortar and passed through a pore size <44 µm sieve on a Pulverisette 5 ball mill (Bruker). The pulverized samples were scanned by a Cu anode from 5° and 70° 2θ with a step size of 0.03° operating at a velocity 1.0 s per step, 30 kV, and 10 mA electric current. Particle size distribution of sediments was measured using the sieve method and by using a particle size analyzer (Analysette 22 Micro Tec plus, Fritsch, Idar-Oberstein, Germany).

3.2. Trace Elements Assessment in Sediment

3.2.1. Sediment Quality Control Guidelines

Guidelines for Environmental and Geochemical Assessment of Sediments in Russia are not currently developed. The exception is the regional standard for the city of St. Petersburg. Therefore, the TE concentrations in the sediment samples were compared to consensus-based sediment quality guidelines (SQGs), which include two effect values—the threshold effect concentration (TEC) and probable quality guidelines (PEC) [71]. TE concentrations below the TEC value indicate that this TE is non-toxic and does not pose a threat to aquatic organisms, whereas values above PEC indicate that this TE is toxic and that harmful effects are likely to be observed. Sediment contamination with TE was also assessed using the Polish Geochemical Classification of Sediments (Table 2 [72]).

Table 2. Classification of sediment quality.

Guidelines	Zn	Cd	Pb	Ni	Cu	Cr	Hg	As
Geochemical quality classes (mg/kg) [72,73]								
Class I	125	0.7	30	16	20	50	0.2	<10
Class II	300	3.5	100	40	100	100	0.7	30
Class III	1000	6	200	50	300	400	0.7	50
Class IV	>1000	>6	>200	>50	>300	>400	>0.7	>50
Sediment quality guidelines (mg/kg) [71]								
TEC	121	0.99	35.8	22.7	31.6	43.3	0.18	9.8
PEC	459	4.98	128	48.6	149	111	1.06	33

The consensus-based PECQ was used in this study to predict sediment toxicity [74]. The mean PEC quotient (PECQ) was calculated for the seven measured TE. Mercury was not included in the calculation of the m-PECQ. The mean PECQ for each sediment sample was calculated as the ratio of each element's concentration to the corresponding PEC [73]. If the mean PECQs were found to be <0.5, sediment samples were non-toxic, indicating a low potential toxicity to benthic fauna, whereas sediment samples with PECQ > 0.5 were predicted to be toxic, indicating a high potential risk for bottom fauna [48,52]. The LAWA classification was also used to assess the quality of sediments [52]. The sediments were classified as follows: first class—unpolluted sediments, second class—moderately polluted sediments, third class—heavily polluted sediments, and fourth class—very heavily polluted sediments.

3.2.2. Contamination Factor (CF) and Pollution Load Index (PLI)

The pollution load index (*PLI*) was proposed by Tommilson et al., (1980) to assess the extent of pollution by TE in sediments as follows Equation (1) [75]:

$$PLI = (CF_{i1} \times CF_{i2} \times \ldots \times CF_{in})^{1/n}, \quad (1)$$

where n is the measured number of TE, CF_n is a contamination factor calculated for each analyzed TE, and sediments with $PLI > 1$ are classified as polluted, while $PLI < 1$ corresponds to no pollution. The CF calculation formula is as follows (2) [76]:

$$CF = C_n / B_n, \quad (2)$$

where C_n and B_n are the measured and background values of each TE, respectively. In our case, the background value was obtained from sampling point R1 prior to acid mine water discharge. Analysis of the results of sediment contamination assessment was applied using the standard CF contamination classification: $CF < 1$ indicates low contamination; $1 < CF < 3$ moderate contamination; $3 < CF < 6$ considerable contamination; and $CF > 6$ very high contamination.

3.2.3. Geoaccumulation Index

The index of geoaccumulation (I_{geo}) was calculated by the equation proposed by (Müller, 1969) as follows (3) [77]:

$$I_{geo} = log_2 (C_n / 1.5B_n), \quad (3)$$

where C_n is the heavy TE concentration in the sediment point, and B_n is the geochemical background concentration of TE obtained from sampling point R1 prior to AMD. The corrector factor of 1.5 is used with possible variations in the background data. The I_{geo} value can be classified into seven classes of pollution of the sediments: class 0 ($I_{geo} \leq 0$), uncontaminated; class 1 ($0 < I_{geo} \leq 1$)—uncontaminated to moderately contaminated; class 2 ($1 < I_{geo} \leq 2$)—moderately contaminated; class 3 ($2 < I_{geo} \leq 3$)—moderately to heavily contaminated; class 4 ($3 < I_{geo} \leq 4$)—heavily contaminated; class 5 ($4 < I_{geo} \leq 5$)—heavily to extremely contaminated; and class 6 ($5 \leq I_{geo}$)—extremely contaminated.

3.2.4. Potential Ecological Risk Index

The potential ecological risk index (RI) was developed by the Swedish scientist Hakanson in 1980 [76]. The calculation formula is as follows (4):

$$\mathrm{RI} = \sum_{i=1}^{n} E_r^i = \sum_{i=1}^{n} (T_r^i \times CF_i), \quad (4)$$

where E_r and T_r are the potential ecological risk factor and the "toxic-response" factor of the TE in sediments, respectively, and CF_n is contamination. The "toxic-response" factors for Hg, Cd, Ni, Cr, Cu, As, Pb, and Zn are 40, 30, 5, 2, 5, 10, 5, and 1, respectively [76]. The potential ecological risk factor and potential ecological risk index are divided into the following categories: low risk ($E_r^i < 40$ and $\mathrm{RI} < 150$), moderate risk ($40 \leq E_r^i < 80$ and $150 \leq \mathrm{RI} < 300$), considerable risk ($80 \leq E_r^i < 160$ and $300 \leq \mathrm{RI} < 600$), high risk ($160 \leq E_r^i < 320$ and $\mathrm{RI} \geq 600$), and very high risk ($320 \leq E_r^i$).

3.3. Ecotoxicity Test

Acute toxicity assessment of sediments was assessed using the crustacean Daphnia magna and green algae Scenedesmus quadricauda Breb. [78,79]. The bioassay had been perfomed using juvenile crustacean at the age of 6–24 h in three parallel series for 96 h. D.magna were fed daily with the algae Scenedesmus quadricauda. Green protococcal algae Scenedesmus quadricauda Breb., in the exponential growth stage (3–5 days after reseeding), were also used for bioassay. The studies were performed in two replicates for 72 h. Bioassay was conducted at 20 ± 2 °C with a photoperiod of 16 h of light:8 h of darkness; illumination was 500–1000 lux. The control was the culture water in which the whole culture lived in the laboratory. An indicator of acute toxic effects of the bottom sediments under study was the mortality more than 50% of D.magna individuals within 96 h and a decrease in the number of Scenedesmus quadricauda Breb. algae cells by more than 20% within 72 h. The relative

(%) change in the number of algae cells for each dilution compared to the control (I) was calculated by Formula (5):

$$I = (X_k - X_s)/X_k \times 100\%, \quad (5)$$

where X_k is the mean value of the test parameter in the control; X_s is the mean value of the test parameter in the experiment; and I is the change in the number of algae cells.

To assess the toxicity of each bioassay, we used the PE toxicity classification system (Percent toxic effect) developed by Persoone et al. (2003): class I—no acute toxicity, PE < 20%; class II—slight acute toxicity, 20% < PE < 50%; class III—toxic, 50% <PE < 100%; class IV—very high acute toxicity, PE = 100% [80].

4. Results and Discussions

4.1. The Particle Size Distribution

Sorption and desorption of pollutants increases in sediments of the smallest fraction as well as with increasing pH due to a larger surface area, improving the toxicity of sediments [81–84]. Figure 5 shows a general overview of particle size in the sediments fraction. All sample points had a silt fraction >70%. A higher percentage of fine-grained sediments (0.50–3.15 µm) was found at the AMD site (R2), which is likely due to sedimentation of iron hydroxide, sulfides, and other minerals with acidic forms of atoms that undergo oxidation. A high sand content was found at sampling point R6. All bay sediments had similar particle size distribution of silt > clay > sand.

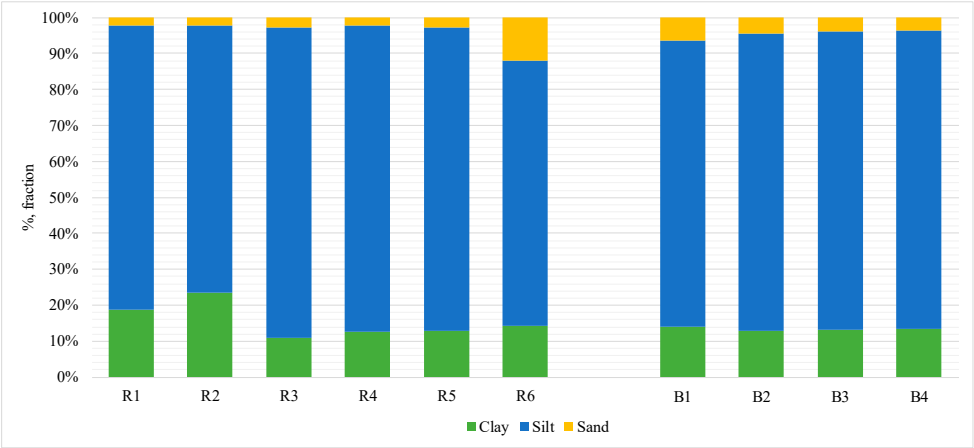

Figure 5. Granulometric composition of sediments.

4.2. Mineralogy

Table 3 shows the main and accessory minerals found in sediments. Based on XRD analysis, quantitatively, the main occurring minerals in river sediment samples were quartz (32–55 wt. %), plagioclase (1–13 wt. %), mica (4–13 wt. %), k-feldspar (7–13 wt. %), chlorite (6–11 wt. %), pyroxene (5–10 wt. %), goethite (3–14 wt. %), hematite (5–11 wt. %), and traces of calcite. In addition to quartz, the main minerals in the area of AMD are goethite and hematite. This area is characterized by the active formation of goethite from amorphous iron-hydroxides in sediments [21].

The presence of calcite and dolomite in river sediments is caused by drainage of carbonate rocks in the Kosva River. The composition of samples from the lower reaches of the river (R6) is close to that of territories outside the AMD effect. The content of goethite is insignificant here (up to 2.6 wt. %). The bay sediments are mainly composed of quartz (35–52 wt. %), clay minerals (12–21 wt. %), plagioclase (9–15 wt. %), k-feldspar (7–13 wt. %), and traces oxides, such as goethite and hematite.

Table 3. Mineral composition of Kosva River and Kosva Bay sediments samples.

Samples	Main Minerals (wt. %)	Accessory Minerals
R1	Quartz (57.0), dolomite (12.7), plagioclase (7.7), mica(6.3), k-feldspar(5.9), pyroxene (4.0), chlorite (3.5)	Calcite, hematite
R2	Quartz (54.7), hematite (11.1),goethite (10.2), k-feldspar (6.9), chlorite (5.8), pyroxene (4.4), mica (4.1)	Calcite, plagioclase
R3	Quartz(39.1), goethite(13.8), mica (12.6), k-feldspar (10.2),chlorite (8.6), pyroxene (7.6), plagioclase (3.6)	Hematite, calcite
R4	Quartz (51.9), k-feldspar (12.2), plagioclase (10.5), pyroxene (7.2), chlorite (7.1), mica (6.7)	Hematite, goethite
R5	Quartz(32.1), k-feldspar (12.1), mica (11.1),goethite (10.9), chlorite (10.5), plagioclase (10.1), pyroxene (9.5)	Calcite, hematite
R6	Quartz(53.0), plagioclase (13.1), k-feldspar (9.2), mica (7.9), chlorite (6.9), pyroxene (5.4)	Goethite, hematite, calcite
B1	Quartz (52.2), plagioclase (13.2), clay minerals (12.4), k-feldspar (12.0), diopside (5.1)	Goethite, hematite
B2	Quartz (51.4), clay minerals(13.5), plagioclase (13.4), k-feldspar (13.4), diopside (5.3)	Goethite, hematite
B3	Quartz (37.5), clay minerals(21.3), k-feldspar (18.8), plagioclase (8.7), diopside(6.8), hematite (5.5)	Goethite
B4	Quartz (34.9), clay minerals (21.4), plagioclase (15.4), k-feldspar (14.2), goethite(7.2), diopside(5.7)	Hematite

4.3. Major Oxides

The major oxide composition of the Kosva River and the Kosva Bay sediments is shown in Figure 6 and Table 4. In general, the dominant oxide form in the sediments of the study area is SiO_2 (42–72 wt. %), followed by Fe_2O_3 and Al_2O_3. The other oxides have much lower average weight percentages. Significant Fe_2O_3 content up to 26.1 wt. % and Al_2O_3 content up to 7.26 wt. % were noted in sediments at AMD sites. This was caused by sedimentation of amorphous hydrated forms of these TE from AMD. The high LOI value for these samples (up to 21.14 wt. %) is primarily associated with crystallized forms of iron precipitation water. Increased content of such oxide forms as CaO and MgO is a reflection of calcite and dolomite content from carbonate rocks of the river catchment area. In the bay sediments, an increase in Al_2O_3 content of up to 14.6 wt. % was noted as well as significant increase of LOI of up to 21.4 wt. %. This was clearly caused by the presence of clay minerals. The Fe_2O_3 content decreased to 10.4 wt. %.

Table 4. Comparison of the chemical composition of sediment samples from this study with the upper continental crust (UCC) [85].

Major (wt. %)	SiO_2	Al_2O_3	Fe_2O_3	K_2O	Na_2O	MgO	CaO	TiO_2	P_2O_5	MnO	SO_3
Kosva River	41.69–72.31	6.65–10.0	6.29–26.1	0.36–1.28	0.29–1.17	0.16–1.34	0.95–1.77	0.48–0.59	0.08–0.98	0.05–0.37	0.02–0.03
Kosva Bay	49.61–64.08	10.31–16.49	7.98–10.36	1.32–1.56	0.62–0.91	1.1–1.81	0.80–1.61	0.57–0.95	0.31–0.72	0.07–0.19	0.02–0.03
UCC	64.9	14.6	4.4	3.5	3.5	2.2	4.1	0.5	0.1	0.07	-

Table 3 shows a comparison of the major oxide data with the Upper Continental Crust (UCC) [85]. In sediments from AMD areas, a significant excess of UCC in Fe_2O_3 content (up to six times) was noted, which was preserved in the Kosva Bay sediments (up to 2.4 times). MnO and P_2O_5 followed the same pattern. After AMD, the average TiO_2 value was higher than the average UCC value, with the highest values in the Kosva Bay sediments.

All sediment samples examined were depleted compared to UCC in terms of the content of other oxides (MgO, Na_2O, K_2O) except for CaO at the background point (R1) and Al_2O_3 (B1).

4.4. Distribution of Trace Elements in Sediments

Table 5 shows the maximum, minimum, and mean values of TE in sediments in the Kosva River and the Kosva Bay. The ranges of TE values in the Kosva River sediments are the following: 31.63 to 100.63 mg/kg (Zn), 25.56 to 39.29 mg/kg (Cu), 8.76 to 131.61 mg/kg (Pb), 37.12 to 48.47 mg/kg (Ni), 77.26 to >4000 mg/kg (Cr), 0.74 to 1.09 mg/kg (Cd), 2.73 to 3.14 mg/kg (As), and 1.01 to 4.62 mg/kg (Hg). The mean concentration of TE in the river sediments corresponded to the following descending sequence: Cr > Ni > Zn > Pb > Cu > As > Hg > Cd. The concentrations of Zn, Cu, and As were found to be higher in the bay sediments than in the river sediments. However, significant Cr concentrations (>4000 mg/kg) were found in sediments upstream of the bay.

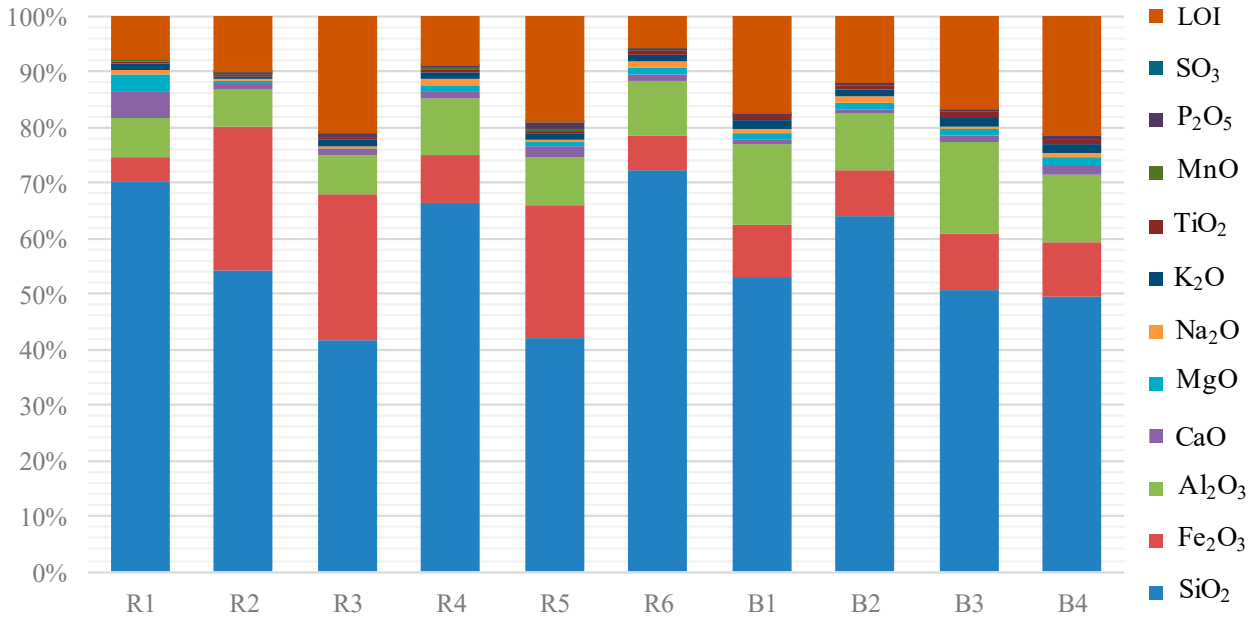

Figure 6. Chemical composition of sediments from the study area.

Table 5. Distribution of TE in sediments of the Kosva River and the Kosva Bay, (mg/kg).

	Kosva River (*n* = 5)			**Kosva Bay (*n* = 4)**		
	Range	**Mean**	**SD**	**Range**	**Mean**	**SD**
Zn	31.63–100.63	61.46	24.86	9.88–207.76	105.98	87.28
Cu	25.56–39.29	33.05	4.86	44.49–78.10	66.69	14.83
Pb	8.76–131.61	36.54	53.47	0.05–30.17	14.63	12.47
Ni	37.12–48.47	41.92	5.69	41.82–82.74	54.70	18.95
Cr	77.26–>4000	1653.33	2142.23	78.24–890.55	288.09	401.77
Cd	0.74–1.09	0.93	0.15	0.02–0.70	0.47	0.32
As	2.73–3.14	2.91	0.14	0.05–10.86	5.73	4.46
Hg	1.01–4.62	2.59	1.55	0.25–3.52	1.44	1.44

The TE content of the Kosva River sediments differs significantly from that of the Kosva Bay. The concentrations of Zn, Cu, Pb, Ni, Cr, Cd, As, and Hg (mg/kg) in the bay sediments ranged as follows: 9.88–207.76 for Zn, 44.49–78.10 for Cu, 0.05–30.17 for Pb, 41.82–82.74 for Ni, 78.24–890.55 for Cr, 0.02–0.70 for Cd, 0.05–10.86 for As, and 0.25–3.52 for Hg. Concentrations of Zn, Cu, Ni, and As are increasing in the bay. Average TE concentrations in the bay sediments decreased in the following order: Cr > Zn > Cu > Ni > Pb > As > Hg > Cd.

4.5. Assessment of Sediment Contamination and Ecological Risk

4.5.1. Contamination Factor and Pollution Load Index

The calculated *PLI* values of TE in sediments are presented in Table 6. The *PLI* values of river sediments ranged from 1.31 at the samples from R4 to 3.60 at the samples from R2 (after discharge acid mine drainage). However, the *PLI* values in bay sediments demonstrated increase from samples from B1 (*PLI* = 1.82) to B4 (*PLI* = 3.83). According to the *PLI* classification [86], river sediments and bay sediments should be classified from moderately unpolluted to unpolluted (1 < *PLI* < 2) to moderately to highly polluted (3 < *PLI* < 4). The contamination factors value analysis (*CF*) indicates that Cr is the TE that has a significant effect on sediment pollution of river sediments to a greater extent than the bay sediments. The contamination factor *CF* calculated for Cr ranged from 0.90 to 46.37, which should be classified from low contamination to very high contamination. Very high contamination in

sediments were found in samples R2 and R6. The contamination factors calculated for other TE ranged from low contamination to moderate contamination. The contamination factors (*CF*) of bay sediments for samples B1–B4 classified from low contamination to very high contamination. Based on mean values of contamination factor of bay sediments identified from low contamination to considerable contamination, Cu and Cr played the largest role in the contamination of the analyzed sediments.

Table 6. Contamination factors and pollution load index values of TE in sediments of Kosva River and Kosva Bay.

Sampling Point	Zn	Cu	Pb	Ni	Cr	Cd	As	Hg	*PLI*
	CF								
R2	0.77	2.14	8.20	1.51	46.37	1.59	1.12	0.43	3.60
R3	1.33	1.90	1.43	1.16	0.98	1.09	1.25	0.14	1.34
R4	1.47	1.64	0.62	1.17	0.90	1.24	1.08	0.32	1.31
R5	2.45	1.86	0.60	1.49	1.21	1.31	1.20	0.12	1.37
R6	1.45	1.44	0.55	1.21	46.37	1.59	1.11	0.56	2.43
B1	3.49	2.44	1.04	1.54	0.91	1.03	2.63	0.09	1.82
B2	1.53	4.25	0.73	1.30	0.95	1.01	2.12	0.42	1.54
B3	5.05	3.93	1.88	2.58	1.18	0.70	4.30	0.15	2.81
B4	0.24	3.89	0.003	1.40	10.32	0.02	0.02	0.03	3.83

4.5.2. Geoaccumulation Index

Figure 7 shows a distribution I_{geo} values (calculated using geochemical background as for *PLI*) for the eight TE in sediments. The highest I_{geo} value (4.95) was for Cr, indicating heavy to extreme contamination at sampling points R2 and R6. The sediment in Kosva Bay was also identified as having the highest value for Cr (2.78) in samples from B4, in which sediment caused moderate to heavy contamination. Lead at sampling point R2 was found in class 3, indicating up to moderate to heavy contamination. The results show that Hg from upstream to downstream, including the bay, have $I_{geo} \leq 0$, indicating an absence of pollution. Other TE Zn, Cu, Ni, and Cd from upstream to downstream had $0 < I_{geo} \leq 1$, indicating lack of contamination to moderate contamination of the sediment. Furthermore, the level of pollution in the bay sediments increased for Zn and Cu up to moderately contaminated.

The pollution levels of the TE in bay sediments are thus segmented into three classes according to the I_{geo} mean value. Thus, sediment in the Kosva Bay is moderately contaminated by Cu (class 2); uncontaminated to moderately contaminated by Cr, Ni, and Zn (class 1); and uncontaminated by Hg, Pb, Cd, and As (class 0).

4.5.3. Potential Ecological Risk Index

The index of potential environmental risk of TE in the sediments of the Kosva River and Kosva Bay is shown in Table 7. Average values of potential ecological risk coefficient (E_r^i) of TE in sediments of the Kosva River decreased in the following order: Cd > Cr > Hg > As > Pb > Cu > Ni > Zn. According to the data, the mean (E_r^i) values of Zn, Cu, Ni, Cr, and Cd ranged between 1.49 and 40.94, demonstrating from low to moderate degree of ecological risk. However, moderate risk was found upstream (R2) and downstream (R6). As shown in Table 7, the values of a single ecological risk index (E_r^i) for Zn, Cu, Pb, Ni, Cr, Cd, and Hg were below 40 in all the sediment samples, suggesting a low ecological risk. Only samples from B4 were determined as posing a moderate risk due to As. The RI of the Kosva River for all sampling points is from 76 to 228, which shows an overall ecological risk level ranging from low to moderate.

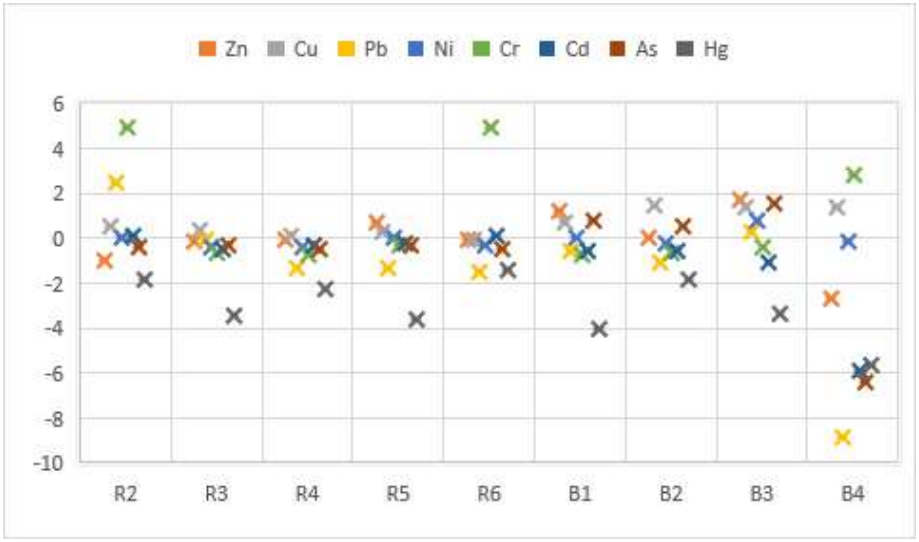

Figure 7. Geoaccumulation index assessment data of TE in sediments.

Table 7. Potential ecological risk assessment results of TE in sediments of the Kosva River and Kosva Bay.

Sampling Point	Unified Environmental Risk Factor Index (E_r^i)								RI	Risk Gradation
	Zn	Cu	Pb	Ni	Cr	Cd	As	Hg		
R2	0.77	10.69	41.00	7.56	92.74	47.64	11.24	17.05	228.69	Moderate
R3	1.33	9.51	7.13	5.79	1.96	32.73	12.46	5.62	76.52	Moderate
R4	1.47	8.21	3.08	5.86	1.79	37.30	10.81	12.62	81.15	Low
R5	2.45	9.31	2.98	7.45	2.43	39.19	11.96	4.86	80.63	Low
R6	1.45	7.22	2.73	6.03	92.74	47.82	11.10	22.27	191.35	Low
Average for R2–R6	1.49	8.99	11.38	6.54	38.33	40.94	11.51	12.48	131.67	Moderate
B1	3.49	12.21	5.18	7.71	1.81	30.97	26.32	3.74	91.42	Low
B2	1.53	21.24	3.64	6.52	1.90	30.18	21.25	16.96	103.22	Moderate
B3	5.05	19.64	9.40	12.90	2.35	21.07	43.04	5.95	119.41	Moderate
B4	0.24	19.47	0.02	6.99	20.65	0.75	0.18	1.19	49.48	Low
Average for B1–B4	2.58	18.14	4.56	8.53	6.68	20.74	22.70	6.96	90.88	Low

4.5.4. Geochemical Quality Classes and LAWA Classification

According to Bojakowska's geochemical quality classes of sediments, all sediment samples taken were classified as class IV (highly contaminated sediments). Classifications were conducted on the basis of the highest concentrations. The concentrations of Zn in B1 and B3 corresponded to class II (slightly contaminated); Pb in R2 to class III (contaminated); Ni in B2 to class IV (highly contaminated); Cr in R2, R6, and B4 to class IV (highly contaminated); Cd in R2–R6 to class II (slightly contaminated); Cd in B3 to class II (slightly contaminated); Hg in all sampling points to class IV (highly contaminated); and Cu in all sampling points (with the exception of R1) to class II (slightly contaminated).

According to the LAWA classification, sediments in sampling points R2, R6, B4, and R1 are heavily contaminated (Figure 8). Comparing the results of geochemical quality classes of sediments to the LAWA classification, we can state that sediments correspond to different classes depending on the concentration of studied chemical elements. As a result, in AMD area, Cr content corresponds to class IV, Hg to class III–IV, and Pb to class II–III.

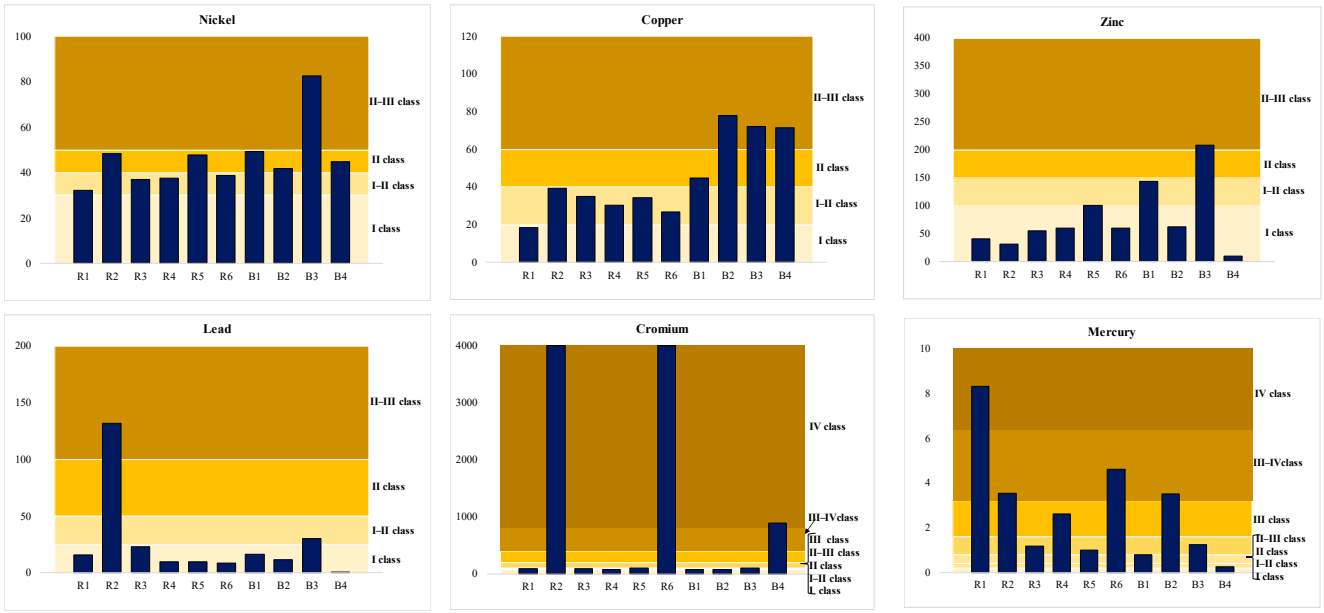

Figure 8. LAWA quality classes for sediments.

Pollution levels of the Kosva Bay sediments varied from contaminated to very heavily contaminated. The highest levels of pollution were found for Cr (IV class) in B4, Hg (III–IV class) in B2, Cu (II–III class) in B2–B4, and Zn and Ni in B3.

4.5.5. Sediment Quality Guidelines

The concentration of TE in the sediment samples of Kosva River and Kosva Bay were compared with the consensus-based TEC and PEC values (Figure 9). The results show that the PEC values were exceeded only in the case of Hg, Cr, Ni, and Pb (80%, 50%, 40%, and 10% of the samples, respectively). Obviously, additional study of the concentration of mercury in sediments in the watershed of the Kosva River and Kosva Bay, where significant concentrations of this element were found in most samples, is necessary according to the data of the present study. Only Cu was detected in all sediment samples between TEC and PEC. At the same time, Cr was found in the Kosva Bay sediments in B3 and B4, Ni in B3 and B1, and Hg in B2 and B3.

The mean PECQ can be used to predict the toxicity of sediments [73]. The highest PECQ values were found in R2 and R6: 5.24 and 5.22, respectively. Mean value of PECQ of six TE was identified for river sediments: PECQ = 2.38, which clearly indicates a significant potential risk for benthic fauna.

In the sediments of Kosva Bay were calculated mean values of PECQ = 0.75 with a range from 0.42 to 1.21. This means that all of the sediment samples were potentially toxic (PECQ > 0.5) [51].

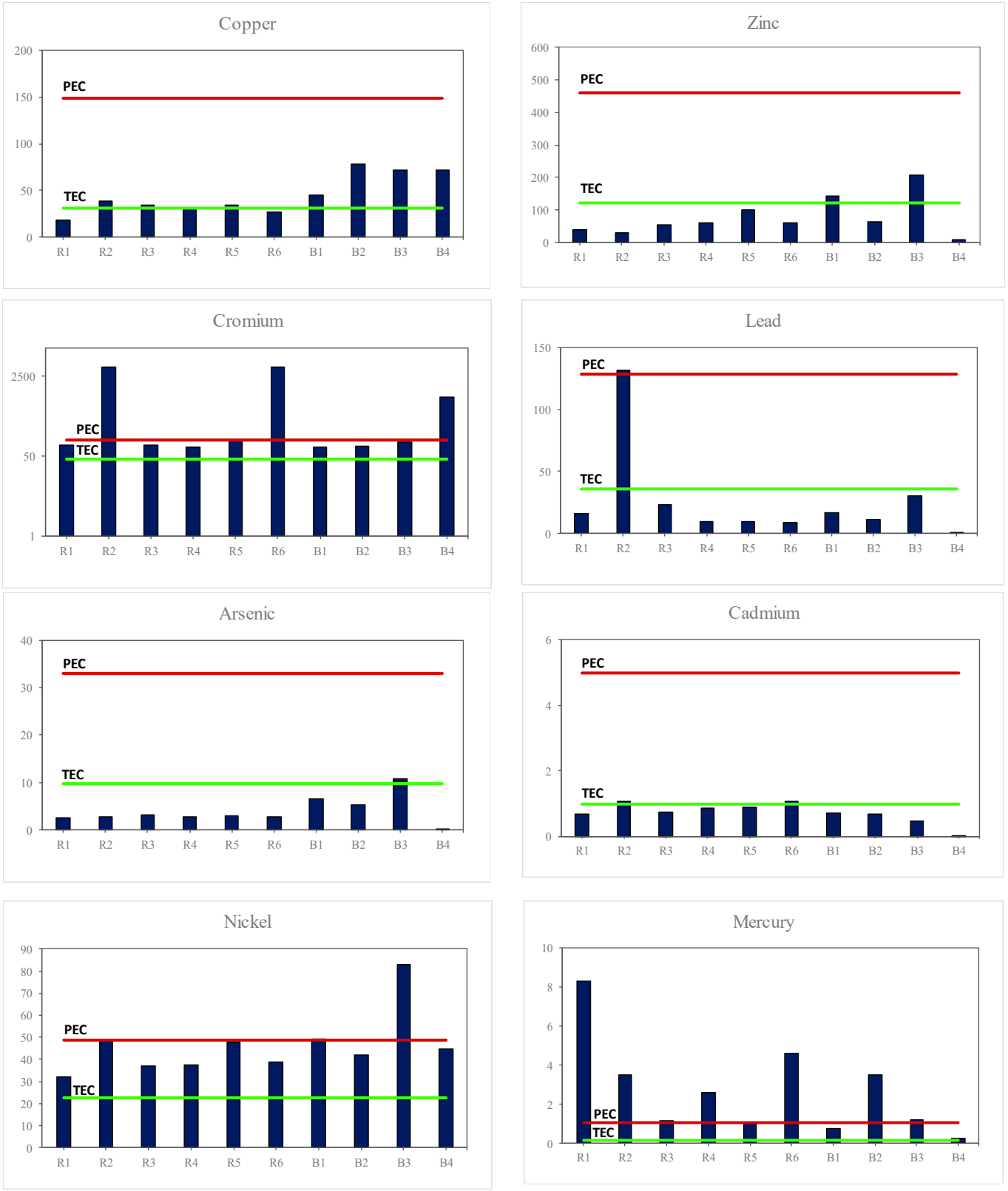

Figure 9. Comparison between TE concentrations (mg/kg) of all samples with sediment quality control guidelines and PEC ratio values (mg/kg).

4.6. Ecotoxicity Test

The results of the sediment toxicity assessment are presented in Tables 8 and 9. Acute toxicity tests using *Daphnia magna* were conducted in sampling point R3 (distance from AMD—2.3 km) and B1 and B4 (Kosva Bay). During the chemical analysis of this water, no aluminum ions were found in its composition (in the measurement range from 0.04 to 0.56 mg/L). The pH level of the tested waters was in the range optimal for crustaceans (7.2–7.8).

Table 8. Ecotoxicity results for the sediments samples using *D. magna*.

Sediment	pH	DO	%Immobility or Dead			Total Alevins Exposed	% Dead Average	Class *	Toxicity
			Assay 1	Assay 2	Assay 3				
R3	7.6–7.74	7.85–7.67	0	0	0	10	0	I	No acute toxicity
B1	6.93–7.55	6.87–6.33	10	10	10	10	0	I	No acute toxicity
B4	7.21–7.49	6.82–6.05	10	10	10	10	0	I	No acute toxicity

* Class: I, no acute PE < 20%; II, slight acute toxicity, 20% < PE < 50%; III, acute toxicity, 50% < PE < 75%; IV, high acute toxicity, 75% < PE < 100%; V, very high acute toxicity, PE > 100%.

Table 9. Results of ecotoxicity for the bay sediments samples using *Scenedesmus quadricauda*.

Sediment	pH	Salinity	EC_{100}, The Number of Algae, Thousand Cells/sm^3		*I*, %	EC_{50}, the Number of Algae, Thousand Cells/sm^3		*I*, %	Toxicity
			Assay 1	Assay 2		Assay 1	Assay 2		
B1	6.83/9.39 *	0.179/0.246 **	26.75	626.25	2,57	29.88	631.25	1.79	No acute toxicity
B4	7.17/9.95	0.198/0.264	25.13	632.20	1,59	31.00	636.25	1.01	No acute toxicity

* pH before testing/pH after testing; ** salinity before testing/salinity after testing.

It was experimentally deduced that a 100% concentration (that is, without dilution of the aqueous extract) caused the death of no more than 10% of *D. magna* within 96 h of the experiment in all studied points. An aqueous extract from sediments did not have an acute toxic effect on the test object *D. magna* at 100% (dilution ratio—1) and all subsequent concentrations.

Similar results were obtained when assessing the bay sediment toxicity using the test object green algae *Scenedesmus quadricauda*. The conducted bioassay showed no toxic effect in sediments from B1 and B4, as the decrease in the number of algae cells of *Scenedesmus quadricauda* was less than 20% within 72 h of the experiment (Table 9).

4.7. Effect of Pollution and Ecotoxicological Indeces on Risk Assessment

Single-element indices (I_{geo} and *CF* values) revealed varying degrees of TE pollution in sediments. The average concentrations of elements in the Kosva Bay sediments decreased in the following order by *CF*: Cu > Cr > Zn > As > Ni > Pb > Cd > Hg; and by I_{geo}: Cu > Cr > Ni > Zn > As > Cd > Pb > Hg. Thus, the average value of *CF* showed that the bay sediments had the highest Cr accumulation (3.3), indicating considerable contamination. Results of the average I_{geo} value calculation showed that the bay sediments had the highest Cu accumulation (1.2), indicating moderate contamination. In comparison to the *CF*, I_{geo} used a factor of 1.5 to minimize the impact of background value. According to Liao et al. [87], I_{geo} appears to be independent of lithological variation and allows for a comparison of the risk of a given heavy metal in different regions. I_{geo} and *CF* are also required to accurately assess heavy metal accumulation from various anthropogenic sources.

In general, the evaluation effects of *PLI* and RI are not equal. All bay sediments had *PLI* values greater than 1. While the average RI value was 90.88, with As contributing the most, E_r^i was 22.70, indicating low risk. In the complex environmental risk assessment of TE in sediments, providing a more holistic evaluation of RI seems to be a better choice [46].

According to the LAWA and Polish Geochemical Classification of Sediments used in this study, the bay sediments have the highest levels of Cr, Ni, and Hg. These geochemical classifications of sediment quality assess the extent of deviation from reference conditions

with no or minimal anthropogenic influence [36]. The excess of PEC by Cr, Ni, and Hg in the bay sediments indicates adverse effects on benthic organisms, confirming the mean PECQ = 0.75. At the same time, the biotesting results indicate no acute toxicity of sediments in the Kosva Bay. Ecotoxicology tests are a useful tool for evaluating the quality of sediments, and their use allows for a more comprehensive risk classification [49]. Bioassays are an efficient, precise, and commonly used biomonitoring tool that is an excellent addition to the comprehensive sediment assessment [48].

4.8. AMD—Comparison with Other Locations and Effect to Sediments

Different chemical compositions of AMD within coal deposits around the world are primarily conditioned by geological structure of a territory. Consequently, priority pollutants (TE and rare earth elements) actively accumulate in sediments. Table 10 shows the AMD composition of coal deposits from around the world in comparison with the data on the Kizel Coal Basin mines. Even within the same coal basin, AMD can vary significantly. This is evidenced by the data from the Kalinin Mine, which has significantly higher concentrations of all TE in AMD compared to the Tayozhnaya Mine.

Table 10. Integrated data by Characterization of Raw AMD (mg/L).

	Kosva River	**Bolshaya Gremyachaya River**	**Mina Stream**	**Sycamore Creek**	**Wingecarribee River**
	Kalinin Mine	**Tayozhnaya Mine**	**Mina 07 Mine**	**Tab-Simco Mine**	**Berrima Mine**
	Russia	**Russia**	**Brazil**	**USA**	**New Zealand**
pH	3.2	3.3	3.9	2.27	6.36
SO_4	4190.24	1891	2780.5	2481	332
Fe	1507.37	603.40	611.38	137	10.94
Al	122.13	31.83	58.4	80	0.04
Mn	12.16	6.084	11.18	33.19	
Co	0.38	0.1743	0.18	-	0.14
Pb	0.081	0.0006	0.41	7.0	
Cd	0.007	0.085	-	1.0	0.0004
Ni	1.85	0.98	-	3.0	0.42
Zn	0.85	17.45	62.65	11.0	1.16
Li	1.16	-		-	0.06
References	[20]	[8]	[11]	[88]	[13]

The sulphate, iron, and aluminum content of AMD from the Kalinin Mine is significantly higher than AMD from other mines, according to rare, published data on coal mines in Brazil, USA, and New Zealand (Table 10). The rest of the TE in AMD from the Kalinin Mine correspond to the published data of other AMD except for the content of Co and Li, which is also significantly higher in the Kalinin Mine.

In general, taking into account the variation in AMD during the year, significant concentrations of Co, Pb, Cd, Ni, Zn, and Li enter the Kosva River basin. At the same time, concentrations of Cr and Pb in sediments of the Kosva River in AMD areas are more significant in comparison to the published data for other basins, and the concentrations of Zn and As are much lower (Table 11). It seems obvious that this is due to corresponding concentrations of these TE in AMD.

Table 11. Integrated data on trace element content in sediments in places of AMD discharge (mg/kg).

	Kosva River	**Mina Stream**	**Shandi River**	**Wollangambe River**
	After All Mines	**Mina 07 Mine**	**Shandi Mine**	**Centennial Coal Mine**
	Russia	**Brazil**	**China**	**Australia**
Cr	2042.31	31.5	39.39	4
Co	20.34	8.8	-	59
Ni	42.79	18.45	-	53
Cu	37.12	19.25	66.06	7
Zn	43.20	257	570.87	91
As	2.99	25.35	23.54	<4
Cd	0.91	1.06	1.37	-
Hg	2.35	-	-	-
Pb	77.24	22.55	46.37	7
References	This study	[11]	[89]	[90]

The most AMD-affected sites had the highest level of pollution and ecotoxicological indices. The low pH value of the discharge mine water resulted in the further dissolution of minerals and release of toxic metals transported downstream TE, which confirmed the findings of numerous studies [91]. The extent of toxic element accumulation in sediments depends on the status of a mine (operational/abandoned), type of deposit, mining and processing methods, hydrological conditions, hydrogeological settings, geology, and climate [87].

An important characteristic of this territory is that the inflow of AMD into the Kosva River basin from abandoned mines of the Kizel Coal Basin is exposed to natural dilution due to the large amount of rainfall. The barrier effect of the Ural Mountains on the territory of the Kizel Coal Basin causes heavy rainfall (for example, during the observed period, it amounted to 772.5 mm). The value of significant surface runoff for this area is combined with low evaporation of moisture, as the average annual temperature in the study area is 0.5 °C. A humid type of climate and flow regulation by the Shirokovsky Reservoir typical for the territory of the Kizel Coal Basin contribute to intensive transport of common mine water pollutants (Fe, Al, Mn, and many trace elements) into the Kosva Bay and subsequently into the Kama River basin.

5. Conclusions

Based on the results described, it can be concluded that the average concentrations of Cu, Cr, Zn, As, and Ni in the sediments of Kosva Bay were higher than the local background. Combined I_{geo}, *PLI*, RI, SQG, and LAWA pollution indicators are a useful tool for the environmental assessment of sediments, as the results show a significant degree of contamination by many trace elements. Generally, I_{geo} showed that Cu had the highest level of contamination, taking into account average values in the bay. High concentrations of Hg, Ni, and Cr are more likely to result in harmful effects on organisms in sediments, according to the SQCG assessment. Based on the LAWA classification, the Kosva Bay sediments correspond to classes II–IV depending on the content of a given element. At the same time, the potential ecological risk index (RI) values showed that the bay sediments had low environmental risk of pollution by the studied TE. This corresponds to the data of the bioassays based on *D. magna* and *Scenedesmus quadricauda*. The results showed the absence of toxicity of the bay sediments despite rather high content of Cr, Pb, Cu, Zn, and As (primarily in terms of *CF*) in sediments in the AMD area, middle flow of the Kosva River, and the Kosva Bay.

Thus, the results of the study of TE concentrations and spatial distribution in sediments of the Kosva Bay of the Kama Reservoir using element-by-element assessment and bioassays confirm the necessity of using an integrated approach to sample study with a combination of chemical and ecotoxicological analyses for such objects. Due to elevated levels of pollution by some indices in sediment samples of the Kosva Bay, future studies should be supplemented with additional TE content and sediments toxicity of the Kama Reservoir, which is located in the zone of influence of the Kosva River flow, primarily in even more distant sections of the old channel.

Author Contributions: Conceptualization, E.U. and E.M.; methodology, E.M. and S.B.; software, P.B.; validation, E.U., E.M. and P.B.; formal analysis, E.U.; investigation, E.M., S.B. and B.O.; resources, B.O.; data curation, P.B.; writing—original draft preparation, E.U., E.M. and P.B.; writing—review and editing, E.U., E.M., S.B. and B.O.; visualization, P.B. and E.U.; supervision, E.M.; project administration, S.B.; funding acquisition, E.M. All authors have read and agreed to the published version of the manuscript.

Funding: This research was funded by RFBR, project No. 19-05-50071 and Ministry of Science and Higher Education of the Russian Federation project No. 2019-0858.

Institutional Review Board Statement: Not applicable.

Informed Consent Statement: Not applicable.

Data Availability Statement: Data can be made available upon request to the corresponding author.

Conflicts of Interest: The authors declare no conflict of interest.

References

1. Wang, Z.; Xu, Y.; Zhang, Z.; Zhang, Y. Review: Acid Mine Drainage (AMD) in Abandoned Coal Mines of Shanxi, China. *Water* **2020**, *13*, 8. [CrossRef]
2. Thisani, S.; Kallon, D.; Byrne, P. Geochemical Classification of Global Mine Water Drainage. *Sustainability* **2020**, *12*, 10244. [CrossRef]
3. Ji, H.; Li, H.; Zhang, Y.; Ding, H.; Gao, Y.; Xing, Y. Distribution and risk assessment of heavy metals in overlying water, porewater, and sediments of Yongding River in a coal mine brownfield. *J. Soils Sediments* **2018**, *18*, 624–639. [CrossRef]
4. Alvarenga, P.; Guerreiro, N.; Simões, I.; Imaginário, M.; Palma, P. Assessment of the Environmental Impact of Acid Mine Drainage on Surface Water, Stream Sediments, and Macrophytes Using a Battery of Chemical and Ecotoxicological Indicators. *Water* **2021**, *13*, 1436. [CrossRef]
5. Zhang, X.; Tang, S.; Wang, M.; Sun, W.; Xie, Y.; Peng, H.; Zhong, A.; Liu, H.; Zhang, X.; Yu, H.; et al. Acid mine drainage affects the diversity and metal resistance gene profile of sediment bacterial community along a river. *Chemosphere* **2019**, *217*, 790–799. [CrossRef] [PubMed]
6. Welch, C.; Barbour, S.L.; Hendry, M.J. The geochemistry and hydrology of coal waste rock dumps: A systematic global review. *Sci. Total Environ.* **2021**, *795*, 148798. [CrossRef]
7. Semenkov, I.; Sharapova, A.; Lednev, S.; Yudina, N.; Karpachevskiy, A.; Klink, G.; Koroleva, T. Geochemical Partitioning of Heavy Metals and Metalloids in the Ecosystems of Abandoned Mine Sites: A Case Study within the Moscow Brown Coal Basin. *Water* **2022**, *14*, 113. [CrossRef]
8. Fetisova, N.F. Study of migration forms of metals in rivers affected by acid mine drainage of the Kizel coal basin. Bulletin of the Tomsk Polytechnic University. *Geo Assets Eng.* **2021**, *332*, 141–152. (In Russian)
9. Maksimovich, N.G.; Pyankov, S.V.; Khayrulina, E.A. Environmental assessment of closed coal mine territory using GIS anal ysis. In Proceedings of the 13th International Mine Water Association Congress, "Mine Water & Circular Economy—A Green Congress", Lappenranta, Finland, 25–30 June 2017.
10. Torre, B.; Borrero-Santiago, A.R.; Fabbri, E.; Guerra, R. Trace metal levels and toxicity in the Huelva Estuary (Spain): A case study with comparisons to historical levels from the past decades. *Environ. Chem. Ecotoxicol.* **2019**, *1*, 12–18. [CrossRef]
11. Campaner, V.P.; Luiz-Silva, W.; Machado, W. Geochemistry of acid mine drainage from a coal mining area and processes controlling metal attenuation in stream waters, southern Brazil. *An. Acad. Bras. Cienc.* **2014**, *86*, 539–554. [CrossRef]
12. Acharya, B.S.; Kharel, G. Acid mine drainage from coal mining in the United States—An overview. *J. Hydrol.* **2020**, *588*, 125061. [CrossRef]
13. Wright, I.A.; Paciuszkiewicz, K.; Belmer, N. Increased water pollution after closure of Australia's longest operating under-ground coal mine: A 13-month study of mine drainage, water chemistry and river ecology. *Water Air Soil Pollut.* **2018**, *229*, 55. [CrossRef]
14. Olds, W.; Weber, P.; Pizey, M.; Pope, J. Acid mine drainage analysis for the Reddale Coal Mine, Reefton, New Zealand. *N. Z. J. Geol. Geophys.* **2016**, *59*, 341–351. [CrossRef]

15. Zakrutkin, V.E.; Gibkov, E.V.; Reshetnyak, O.S.; Reshetnyak, V.N. River Sediments as River Waters' Primary Pollution Indi-cator and Secondary Pollution Source in East Donbass Coal-Mining Areas. *Bull. Russ. Acad. Sci. Geogr.* **2020**, *84*, 259–271.
16. Younger, P. Mine water pollution in Scotland: Nature, extent and preventative strategies. *Sci. Total Environ.* **2001**, *265*, 309–326. [CrossRef]
17. Galhardi, J.A.; Bonotto, D.M. Hydrogeochemical features of surface water and groundwater contaminated with acid mine drainage (AMD) in coal mining areas: A case study in southern Brazil. *Environ. Sci. Pollut. Res.* **2016**, *23*, 18911–18927. [CrossRef]
18. Pyankov, S.V.; Maximovich, N.G.; Khayrulina, E.A.; Berezina, O.A.; Shikhov, A.N.; Abdullin, R.K. Monitoring Acid Mine Drainage's Effects on Surface Water in the Kizel Coal Basin with Sentinel-2 Satellite Images. *Mine Water Environ.* **2021**, *40*, 606–621. [CrossRef]
19. Xu, J.; Chen, Y.; Zheng, L.; Liu, B.; Liu, J.; Wang, X. Assessment of Heavy Metal Pollution in the Sediment of the Main Tributaries of Dongting Lake, China. *Water* **2018**, *10*, 1060. [CrossRef]
20. Geoenvironmental Geoinformation System of the Kizel Coal Basin. Available online: http://kub.maps.psu.ru (accessed on 11 October 2021). (In Russian).
21. Menshikova, E.; Osovetsky, B.; Blinov, S.; Belkin, P. Mineral Formation under the Influence of Mine Waters (The Kizel Coal Basin, Russia). *Minerals* **2020**, *10*, 364. [CrossRef]
22. Nieto, J.M.; Sarmiento, A.M.; Olías, M.; Canovas, C.R.; Riba, I.; Kalman, J.; Delvalls, T.A. Acid mine drainage pollution in the Tinto and Odiel rivers (Iberian Pyrite Belt, SW Spain) and bioavailability of the transported metals to the Huelva Estuary. *Environ. Int.* **2007**, *33*, 445–455. [CrossRef]
23. Adamovic, D.; Ishiyama, D.; Dordievski, S.; Ogawa, Y.; Stevanovic, Z.; Kawaraya, H.; Sato, H.; Obradovic, L.; Marinkovic, V.; Petrovic, J.; et al. Estimation and comparison of the environmental impacts of acid mine drainage-bearing river water in the Bor and Majdanpek porphyry copper mining areas in Eastern Serbia. *Resour. Geol.* **2021**, *71*, 123–143. [CrossRef]
24. Report "On the State and Environmental Protection of the Perm Territory in 2020". Available online: http://www.permecology.ru (accessed on 23 November 2021). (In Russian).
25. Sojka, M.; Jaskuła, J.; Siepak, M. Heavy Metals in Bottom Sediments of Reservoirs in the Lowland Area of Western Poland: Concentrations, Distribution, Sources and Ecological Risk. *Water* **2018**, *11*, 56. [CrossRef]
26. Kowalska, J.B.; Mazurek, R.; Gąsiorek, M.; Zaleski, T. Pollution indices as useful tools for the comprehensive evaluation of the degree of soil contamination–A review. *Environ. Geochem. Health* **2018**, *40*, 2395–2420. [CrossRef]
27. Weissmannová, H.D.; Pavlovský, J. Indices of soil contamination by heavy metals—Methodology of calculation for pollution assessment (minireview). *Environ. Monit. Assess.* **2017**, *189*, 616. [CrossRef]
28. Liao, J.; Cui, X.; Feng, H.; Yan, S. Environmental Background Values and Ecological Risk Assessment of Heavy Metals in Watershed Sediments: A Comparison of Assessment Methods. *Water* **2021**, *14*, 51. [CrossRef]
29. Dey, M.; Akter, A.; Islam, S.; Dey, S.C.; Choudhury, T.R.; Fatema, K.J.; Begum, B.A. Assessment of contamination level, pollution risk and source apportionment of heavy metals in the Halda River water, Bangladesh. *Heliyon* **2021**, *7*, e08625. [CrossRef]
30. Wojciechowska, E.; Nawrot, N.; Walkusz-Miotk, J.; Matej-Łukowicz, K.; Pazdro, K. Heavy Metals in Sediments of Urban Streams: Contamination and Health Risk Assessment of Influencing Factors. *Sustainability* **2019**, *11*, 563. [CrossRef]
31. Leão, L.; da Costa, R.; Leite, M.; Júnior, H.N.; Fonseca, R. Distribution and Assessment of Trace Elements Contamination in Sediments of Conceição River Basin, Brazil. *Geosciences* **2021**, *11*, 236. [CrossRef]
32. Custodio, M.; Fow, A.; Chanamé, F.; Orellana-Mendoza, E.; Peñaloza, R.; Alvarado, J.C.; Cano, D.; Pizarro, S. Ecological Risk Due to Heavy Metal Contamination in Sediment and Water of Natural Wetlands with Tourist Influence in the Central Region of Peru. *Water* **2021**, *13*, 2256. [CrossRef]
33. Miao, X.; Song, M.; Xu, G.; Hao, Y.; Zhang, H. The Accumulation and Transformation of Heavy Metals in Sediments of Liujiang River Basin in Southern China and Their Threatening on Water Security. *Int. J. Environ. Res. Public Health* **2022**, *19*, 1619. [CrossRef]
34. Nawrot, N.; Wojciechowska, E.; Mohsin, M.; Kuittinen, S.; Pappinen, A.; Rezania, S. Trace Metal Contamination of Bottom Sediments: A Review of Assessment Measures and Geochemical Background Determination Methods. *Minerals* **2021**, *11*, 872. [CrossRef]
35. Acharjee, A.; Ahmed, Z.; Kumar, P.; Alam, R.; Rahman, M.S.; Simal-Gandara, J. Assessment of the Ecological Risk from Heavy Metals in the Surface Sediment of River Surma, Bangladesh: Coupled Approach of Monte Carlo Simulation and Multi-Component Statistical Analysis. *Water* **2022**, *14*, 180. [CrossRef]
36. Khan, S.; Naushad, M.; Lima, E.C.; Zhang, S.; Shaheen, S.M.; Rinklebe, J. Global soil pollution by toxic elements: Current status and future perspectives on the risk assessment and remediation strategies—A review. *J. Hazard. Mater.* **2021**, *417*, 126039. [CrossRef] [PubMed]
37. Zhou, Z.; Wang, Y.; Teng, H.; Yang, H.; Liu, A.; Li, M.; Niu, X. Historical Evolution of Sources and Pollution Levels of Heavy Metals in the Sediment of the Shuanglong Reservoir, China. *Water* **2020**, *12*, 1855. [CrossRef]
38. Cui, S.; Zhang, F.; Hu, P.; Hough, R.; Fu, Q.; Zhang, Z.; An, L.; Li, Y.-F.; Li, K.; Liu, D.; et al. Heavy Metals in Sediment from the Urban and Rural Rivers in Harbin City, Northeast China. *Int. J. Environ. Res. Public Health* **2019**, *16*, 4313. [CrossRef]
39. Pejman, A.; Bidhendi, G.N.; Ardestani, M.; Saeedi, M.; Baghvand, A. A new index for assessing heavy metals contamination in sediments: A case study. *Ecol. Indic.* **2015**, *58*, 365–373. [CrossRef]
40. Bruce, P.; Sobek, A.; Ohlsson, Y.; Bradshaw, C. Risk assessments of contaminated sediments from the perspective of weight of evidence strategies—A Swedish case study. *Hum. Ecol. Risk Assess. Int. J.* **2021**, *27*, 1366–1387. [CrossRef]

41. Aradpour, S.; Noori, R.; Tang, Q.; Bhattarai, R.; Hooshyaripor, F.; Hosseinzadeh, M.; Haghighi, A.T.; Klöve, B. Metal contamination assessment in water column and surface sediments of a warm monomictic man-made lake: Sabalan Dam Reservoir, Iran. *Water Policy* **2020**, *51*, 799–814. [CrossRef]
42. Tarnawski, M.; Baran, A. Use of Chemical Indicators and Bioassays in Bottom Sediment Ecological Risk Assessment. *Arch. Environ. Contam. Toxicol.* **2018**, *74*, 395–407. [CrossRef]
43. Ali, B.N.M.; Lin, C.Y.; Cleophas, F.; Abdullah, M.H.; Musta, B. Assessment of heavy metals contamination in Mamut river sediments using sediment quality guidelines and geochemical indices. *Environ. Monit. Assess.* **2014**, *187*, 1–11. [CrossRef]
44. Carrillo, K.C.; Rodríguez-Romero, A.; Tovar-Sánchez, A.; Ruiz-Gutiérrez, G.; Fuente, J.R.V. Geochemical baseline establishment, contamination level and ecological risk assessment of metals and As in the Limoncocha lagoon sediments, Ecuadorian Amazon region. *J. Soils Sediments* **2021**, *22*, 293–315. [CrossRef]
45. Saleh, A.H.; Gad, M.; Khalifa, M.M.; Elsayed, S.; Moghanm, F.S.; Ghoneim, A.M.; Danish, S.; Datta, R.; Moustapha, M.E.; El-Safa, M.M.A. Environmental Pollution Indices and Multivariate Modeling Approaches for Assessing the Potentially Harmful Elements in Bottom Sediments of Qaroun Lake, Egypt. *J. Mar. Sci. Eng.* **2021**, *9*, 1443. [CrossRef]
46. Izah, S.C.; Richard, G.; Aigberua, A.O.; Ekakitie, O. Variations in reference values utilized for the evaluation of complex pollution indices of potentially toxic elements: A critical review. *Environ. Chall.* **2021**, *5*, 100322. [CrossRef]
47. Santos, J.I.; Vidal, T.; Gonçalves, F.J.; Castro, B.B.; Pereira, J.L. Challenges to water quality assessment in Europe—Is there scope for improvement of the current Water Framework Directive bioassessment scheme in rivers? *Ecol. Indic.* **2021**, *121*, 107030. [CrossRef]
48. Kolarova, N.; Napiórkowski, P. Trace elements in aquatic environment. Origin, distribution, assessment and toxicity effect for the aquatic biota. *Ecohydrol. Hydrobiol.* **2021**, *21*, 655–668. [CrossRef]
49. Heise, S.; Babut, M.; Casado, C.; Feiler, U.; Ferrari, B.J.D.; Marziali, L. Ecotoxicological testing of sediments and dredged material: An overlooked opportunity? *J. Soils Sediments* **2020**, *20*, 4218–4228. [CrossRef]
50. Olkova, A.S.; Berezin, G. "Battery of Bioassays" for Diagnostics of Toxicity of Natural Water when Pollution with Aluminum Compounds. *J. Ecol. Eng.* **2021**, *22*, 195–199. [CrossRef]
51. Boguta, P.; Skic, K.; Baran, A.; Szara-Bąk, M. The influence of the physicochemical properties of sediment on the content and ecotoxicity of trace elements in bottom sediments. *Chemosphere* **2021**, *287*, 132366. [CrossRef]
52. Baran, A.; Tarnawski, M. Assessment of heavy metals mobility and toxicity in contaminated sediments by sequential extraction and a battery of bioassays. *Ecotoxicology* **2015**, *24*, 1279–1293. [CrossRef]
53. Baran, A.; Tarnawski, M.; Koniarz, T. Spatial distribution of trace elements and ecotoxicity of bottom sediments in Rybnik reservoir, Silesian-Poland. *Environ. Sci. Pollut. Res.* **2016**, *23*, 17255–17268. [CrossRef]
54. Opekunov, A.Y.; Mitrofanova, E.S.; Spassky, V.V.; Opekunova, M.G.; Sheinerman, N.A.; Chernyshova, A.V. Chemical composition and toxicity of bottom sediments of small streams of St. Petersburg. *Water Resour.* **2020**, *47*, 196–207. [CrossRef]
55. Sarmiento, A.M.; DelValls, A.; Nieto, J.M.; Salamanca, M.J.; Caraballo, M.A. Toxicity and potential risk assessment of a river polluted by acid mine drainage in the Iberian Pyrite Belt (SW Spain). *Sci. Total Environ.* **2011**, *409*, 4763–4771. [CrossRef]
56. Soucek, D.J.; Cherry, D.S.; Trent, G.C. Relative Acute Toxicity of Acid Mine Drainage Water Column and Sediments to Daphnia magna in the Puckett's Creek Watershed, Virginia, USA. *Arch. Environ. Contam. Toxicol.* **2000**, *38*, 305–310. [CrossRef]
57. Yim, J.H.; Kim, K.-W.; Kim, S.D. Effect of hardness on acute toxicity of metal mixtures using Daphnia magna: Prediction of acid mine drainage toxicity. *J. Hazard. Mater.* **2006**, *138*, 16–21. [CrossRef]
58. Lee, S.-H.; Kim, I.; Kim, K.-W.; Lee, B.-T. Ecological assessment of coal mine and metal mine drainage in South Korea using Daphnia magna bioassay. *SpringerPlus* **2015**, *4*, 518. [CrossRef]
59. Imaykin, A.K. Assessment and Forecast of Hydrogeological Conditions in the Territory of the Kizelovsky Coal Basin after the Closure of Mines. Ph.D. Thesis, Perm State National Research University, Perm, Russia, 2012. (In Russian)
60. Maksimovich, N.G.; Pyankov, S.V. *Kizel Coal Basin: Environmental Problems and Solutions: A Monograph*; Perm State National Research University: Perm, Russia, 2018; 288p. (In Russian)
61. Imaykin, A.K.; Imaykin, K.K. *Hydrogeological Conditions of Kizel Coal Basin during and after Its Operation, Forecast of Their Changes: Monograph*; Perm State National Research University: Perm, Russia, 2013; p. 112. (In Russian)
62. Ivantsov, A.Y.; Razumovskiy, A.A.; Zakrevskaya, M.A. *Upper Vendian Macrofossils of Eastern Europe. Middle and Southern Urals*; PIN RAS Publisher: Moscow, Russia, 2018; p. 190. (In Russian)
63. Grazhdankin, D.; Maslov, A. The room for the Vendian in the International Chronostratigraphic Chart. *Russ. Geol. Geophys.* **2015**, *56*, 549–559. [CrossRef]
64. Grazhdankin, D.V.; Maslov, A.V.; Krupenin, M.T. Structure and depositional history of the Vendian Sylvitsa Group in the western flank of the Central Urals. *Strat. Geol. Correl.* **2009**, *17*, 476–492. [CrossRef]
65. Lozovsky, V.R.; Minikh, M.G.; Grunt, T.A.; Kukhtinov, D.A.; Ponomarenko, A.G.; Sukacheva, I.D. The Ufimian Stage of the East European scale: Status, validity, and correlation potential. *Strat. Geol. Correl.* **2009**, *17*, 602–614. [CrossRef]
66. Benton, M. No gap in the Middle Permian record of terrestrial vertebrates. *Geology* **2012**, *40*, 339–342. [CrossRef]
67. Plyusnin, A.V.; Sulima, A.I.; Timofeev, V.D.; Koval, D.V.; Dementyeva, K.V. Lithological-facial structure of the Ufimian sediments in the central part of the Perm Krai. *Geo Assets Eng.* **2021**, *332*, 29–50.
68. Kotlyar, G.V. Permian sections of southern Primorye: A link in correlation of stage units in the standard and general strati-graphic scales. *Russ. J. Pac. Geol.* **2015**, *9*, 254–273. [CrossRef]

69. Lucas, S.G.; Shen, S.-Z. The Permian chronostratigraphic scale: History, status and prospectus. *Geol. Soc. Lond. Spéc. Publ.* **2018**, *450*, 21–50. [CrossRef]
70. Imaykin, A.K. Forecast of changes in underground and mine water regime in the territory of the Kizel Coal Basin. *Internetnewsletter VolgGASU. Ser. Polythematic* **2012**, *22*, 1–7.
71. MacDonald, D.D.; Ingersoll, C.G.; Berger, T.A. Development and Evaluation of Consensus-Based Sediment Quality Guidelines for Freshwater Ecosystems. *Arch. Environ. Contam. Toxicol.* **2000**, *39*, 20–31. [CrossRef]
72. Bojakowska, I. Criteria for evaluation of water sediments pollution. *Pol. Geol. Rev.* **2001**, *49*, 213–219.
73. Kulbat, E.; Sokołowska, A. Methods of Assessment of Metal Contamination in Bottom Sediments (Case Study: Straszyn Lake, Poland). *Arch. Environ. Contam. Toxicol.* **2019**, *77*, 605–618. [CrossRef]
74. Ingersoll, D.D.M.C.G.; MacDonald, D.D.; Wang, N.; Crane, J.L.; Field, L.J.; Haverland, P.S.; Kemble, N.E.; Lindskoog, R.A.; Severn, C.; Smorong, D.E. Predictions of Sediment Toxicity Using Consensus-Based Freshwater Sediment Quality Guidelines. *Arch. Environ. Contam. Toxicol.* **2001**, *41*, 8–21. [CrossRef]
75. Tomlinson, D.L.; Wilson, J.G.; Harris, C.R.; Jeffrey, D.W. Problems in the assessment of heavy-metal levels in estuaries and the formation of a pollution index. *Helgoländer Meeresunt.* **1980**, *33*, 566–575. [CrossRef]
76. Håkanson, L. An ecological risk index for aquatic pollution control. A sedimentological approach. *Water Res.* **1980**, *14*, 975–1001. [CrossRef]
77. Müller, G. Index of geoaccumulation in sediments of the Rhine River. *GeoJournal* **1969**, *2*, 108–118.
78. Federal Register FR 1 39.2007.03222. *Methodology for Determining the Toxicity of Water and Water Extracts from Soils, Sewage Sludge, and Waste by Mortality and Changes in Fertility of Daphnias*; Akvaros: Moscow, Russia, 2007; 51p.
79. Federal Register FR 1 39.2007.03223. *Methodology for Determining the Toxicity of Water and Aqueous Extracts from Soils, Sewage Sludge, Waste by Mortality and Changes in Chlorophyll Fluorescence Levels and Algae Cell Numbers*; Akvaros: Moscow, Russia, 2007; 48p.
80. Persoone, G.; Marsalek, B.; Blinova, I.; Törökne, A.; Zarina, D.; Manusadzianas, L.; Nalecz-Jawecki, G.; Tofan, L.; Stepanova, N.; Tothova, L.; et al. A practical and user-friendly toxicity classification system with microbiotests for natural waters and wastewaters. *Environ. Toxicol.* **2003**, *18*, 395–402. [CrossRef] [PubMed]
81. Singh, P.; Nel, A.; Durand, J. The use of bioassays to assess the toxicity of sediment in an acid mine drainage impacted river in Gauteng (South Africa). *Water SA* **2017**, *43*, 673. [CrossRef]
82. Dauvalter, V.A. *Geoecology of Lake Sediments*; Murmansk STU Publisher: Murmansk, Russia, 2012; p. 242. (In Russian)
83. Copaja, S.V.; Mauro, L.; Vega-Retter, C.; Véliz, D. Adsorption-desorption of Trace Elements in Sediments of the Maipo River Basin. *J. Chil. Chem. Soc.* **2020**, *65*, 4778–4783. [CrossRef]
84. Erguler, Z.A.; Erguler, G.K. The effect of particle size on acid mine drainage generation: Kinetic column tests. *Miner. Eng.* **2015**, *76*, 154–167. [CrossRef]
85. Wedepohl, H.K. The composition of the continental crust. *Geochim. Cosmochim. Acta* **1995**, *59*, 1217–1232. [CrossRef]
86. Zhu, Z.; Xue, J.; Deng, Y.; Chen, L.; Liu, J. Trace metal contamination in surface sediments of intertidal zone from Qinhuangdao, China, revealed by geochemical and magnetic approaches: Distribution, sources, and health risk assessment. *Mar. Pollut. Bull.* **2016**, *105*, 422–429. [CrossRef] [PubMed]
87. Ray, S.; Dey, K. Coal Mine Water Drainage: The Current Status and Challenges. *J. Inst. Eng. Ser. D* **2020**, *101*, 165–172. [CrossRef]
88. Roychowdhury, A.; Sarkar, D.; Datta, R. Removal of Acidity and Metals from Acid Mine Drainage-Impacted Water using Industrial Byproducts. *Environ. Manag.* **2019**, *63*, 148–158. [CrossRef]
89. Chen, D.; Feng, Q.; Li, W.; Song, Y.; Zhao, C. Effects of acid drainage from abandoned coal mines on the microbial community of Shandi River sediment, Shanxi Province. *Int. J. Coal Sci. Technol.* **2021**, *8*, 756–766. [CrossRef]
90. Ali, A.; Strezov, V.; Davies, P.J.; Wright, I.A.; Kan, T. Impact of coal mining on river sediment quality in the Sydney basin, Australia. *Int. J.Environ.Chem.Ecol. Geol. Geophys. Eng.* **2017**, *11*, 243–248.
91. Luís, A.T.; Córdoba, F.; Antunes, C.; Loayza-Muro, R.; Grande, J.A.; Silva, B.; Diaz-Curiel, J.; da Silva, E.F. Extremely Acidic Eukaryotic (Micro) Organisms: Life in Acid Mine Drainage Polluted Environments—Mini-Review. *Int. J. Environ. Res. Public Health* **2021**, *19*, 376. [CrossRef] [PubMed]